Magnetic Resonance Imaging 61 (2019) 267–272

Contents lists available at ScienceDirect

Magnetic Resonance Imaging

journal homepage: www.elsevier.com/locate/mri

Original contribution

MRI imaging and histopathological study of brain iron overload of β-thalassemic mice

Paranee Yatmark[a,*], Somkiat Huaijantug[b], Wuttiwong Teerapan[c], Saovaros Svasti[d], Suthat Fucharoen[d], Noppawan Phumala Morales[e]

[a] Department of Pre-clinic and Applied Animal Science, Faculty of Veterinary Science, Mahidol University, Nakorn Pathom, Thailand
[b] Department of Clinical Sciences and Public Health, Faculty of Veterinary Science, Mahidol University, Nakorn Pathom, Thailand
[c] Department of Companion Animals Clinical Sciences, Faculty of Veterinary Medicine, Kasetsart University, Bangkok, Thailand
[d] Institute of Molecular Biosciences, Mahidol University, Nakorn Pathom, Thailand
[e] Department of Pharmacology, Faculty of Science, Mahidol University, Bangkok, Thailand

ARTICLE INFO

Keywords:
Brain iron overload
Brain pathology
Deferiprone
Beta-thalassemic mice
Magnetic resonance imaging

ABSTRACT

Brain iron overload is chronic and slow progressing and plays an important role in the pathogenesis of neurodegenerative disorders. Magnetic resonance imaging (MRI) is a useful noninvasive tool for determining liver iron content, but it has not been proven to be adequate for evaluating brain iron overload. We evaluated the usefulness of MRI-derived parameters to determine brain iron concentration in β-thalassemic mice and the effects of the membrane permeable iron chelator, deferiprone. Sixteen β-thalassemic mice underwent 1.5 T MRI of the brain that included a multiecho T2*-weighted sequence. Brain T2* values ranged from 28 to 31 ms for thalassemic mice. For the iron overloaded thalassemic mice, brain T2* values decreased, ranging from 8 to 12 ms, which correlated with the iron overload status of the animals. In addition, brain T2* values increased in the group with the treatment of deferiprone, ranging from 18 to 24 ms. Our results may be useful to understand brain pathology in iron overload. Moreover, data could lead to an earlier diagnosis, assist in following disease progression, and demonstrate the benefits of iron chelation therapy.

1. Introduction

Brain iron accumulation, an initial cause of neuronal death, has been reported in neurodegenerative diseases and inflammation of the central nervous system, including Parkinson's disease, Alzheimer diseases, and neuroferritinopathy [1,2]. Previous studies have shown that iron overload accelerates cognitive impairment in a transgenic mice model of Alzheimer's disease [3]. Abnormal increases of iron only occurred in some specific regions of the brain of patients with neurodegenerative disorders [4]. Brain iron overload is associated with worse cognitive performance in obese subjects [5]. Neurodegeneration that results from iron toxicity can lead to apoptosis and ferroptosis, an iron-specific form of nonapoptotic cell death [6,7].

In β-thalassemia patients, iron accumulates to excessive levels in different parts of the body and is cytotoxic. Locations primarily include the liver, heart, pituitary gland, and pancreas, and this accumulation may cause organ dysfunction [8]. Previous studies have shown that only one study assessed iron in the brain of young thalassemia patients by MRI. The study showed significantly higher R2 values in the cortex, the putamen and the caudate nucleus of patients than in the controls [9]. Increased iron deposition in the anterior pituitary gland is the cause of hypogonadotropic hypogonadism and growth hormone deficiency [10]. Gonadotropin cell death due to iron toxicity is probably the cause of the decreased pituitary gland height observed in thalassemia patients with hypogonadotropic hypogonadism [11].

MRI has long been considered a useful noninvasive tool for evaluating iron overload in organs [12]. In the human brain, over the last two decades, iron deposition in tissues has led to signal changes in T2*-weighted MR images [13]. MRI for iron overload was first used in hemochromatosis, one of the most frequent diffuse liver diseases. Since then, MRI has widely replaced biopsies when investigating liver iron overload. MRI has been mainly used to evaluate brain iron accumulation in multiple sclerosis [14] and neurodegenerative diseases including Alzheimer's and Parkinson's disease [15–17].

In this study, we used the model of iron overload in β-thalassemic mice to apply and develop an MRI technique to study the anatomy and pathology of the brain and observe the effect of iron chelation. Therefore, the present study aimed to investigate iron accumulation in

* Corresponding author.
E-mail address: paranee.yat@mahidol.edu (P. Yatmark).

https://doi.org/10.1016/j.mri.2019.05.022
Received 5 November 2018; Received in revised form 17 May 2019; Accepted 19 May 2019

the brain of β-thalassemic mice using an MRI technique. The results of the MRI may demonstrate the distribution of iron in the brain and correlate with the iron overload status of the animals. Additionally, the effects of the membrane permeable iron chelator, deferiprone, will be studied. The results from this study may help to understand brain pathology in iron overload and the benefits of iron chelation therapy.

2. Materials and methods

2.1. Animals

Male and female heterozygous β-globin knockout mice ($^{mu}\beta^{th3/+}$, BKO) 7 weeks of age and weighing 17–25 g were obtained from the Thalassemia Research Center, Institute of Science and Technology for Research and Development, Mahidol University, Thailand. β-globin gene knockout was produced by heterozygous deletion of both β^{major} and β^{minor} on chromosome 7 of mice, leading to β-globin deficiency. As a result, mice developed pathological and clinical signs resemble β-thalassemia intermedia in human [18,19]. Mice were acclimatized for 1 week before the experiments and were housed under conventional sterile conditions. The rodent diet (082G/15) and water were provided *ad libitum*. The temperature and humidity were maintained at 25 ± 2 °C and 60 ± 5%, respectively, and the animals were kept on a 12 h light/dark cycle. The protocol used in this study was approved by the Faculty of Veterinary Science-Animal Care and Use Committee, Mahidol University of Thailand (MUVS-2016-03-10).

2.2. Experimental design and preparation for imaging

BKO mice will be divided into 3 groups: group A: control group (0.9% NaCl), group B: iron overloaded group and group C: iron overloaded with iron chelator, deferiprone. Iron overload was induced by intraperitoneally (i.p.) injection of iron dextran (Sigma, St. Louis, MO, USA) at a dose of 20 mg iron/mouse for a period of 5 days for a total iron administration of 100 mg/mouse in group B and C. Three days after the last dose of iron dextran, iron overloaded group B was i.p. injected with 0.9% NaCl and group C was i.p. injected with 80 mg/kg/day deferiprone (L1, The Government Pharmaceutical Organization, Bangkok, Thailand) for 7 days. After completion of drug treatments, the mice were performed MRI scanning [20]. For MRI scanning the mice were anesthetized with an i.p. injection of thiopental (Nembutal®) (50 mg/kg, Ceva Santé Animale, Libourne, France). All mice were still alive after scanning, and then sacrificed immediately after MRI scan. Brain tissues were collected for determination of brain iron content and histopathological study.

3. Methods

3.1. MRI scanning

MR images of brain were acquired using a 1.5 T Siemens Magnetom (Siemens AG, Medizinische Technik, Germany). The MRI protocol was determined using a modification of the method described by Grabill et al. [20]. Images were acquired using an 8-channel wrist coil and multi-channel receiver, built to conform to the shape of the mouse's skull to optimize signal to noise over the entire mouse brain. MR methods for assessing tissue iron including: (a) method for evaluating histogram analyses based on T2-weighted image with the following parameters: field of view (FOV) = 69.5 mm; matrix size = 125 × 256; slice thickness = 1.6 mm; voxel size = 0.6 × 0.4 × 1.6 mm; repetition time (TR) = 2000 ms; TE = 82 ms (b) method for calculating T2* values: the multiecho fast gradient echo sequence: FOV = 35 mm; matrix size = 45 × 128; slice thickness = 3 mm; voxel size = 0.8 × 0.6 × 3.0 mm; TR = 400 ms; interecho time (TE1-TE8) = 4.4, 7.43, 10.46, 13.49, 16.52, 19.55, 22.58, and 25.61 ms; and number of echoes = 8. Total scan acquisition time was on the order of 20 min. [20]. All scans were reported at the time of acquisition by multiple operators.

3.2. Brain MRI: quantitative histogram analyses and T2* values

Histogram analysis of signal intensity values generated using the OsiriX histogram tool. Brain histogram analyses calculated from T2 weighted images of the 3 brain regions including cortex-cerebellar white matter, superior colliculus, and hippocampus were determined by manually tracing the 3 brain regions on each slice using a Dicom Viewer (OsiriX, The OsiriX Foundation, Geneva, Switzerland). The total mean histogram analysis of the regions was calculated from each slice in all mice. The methods for histogram analysis were modified from Della Nave et al. and Blackledge et al. [21,22].

All the brain T2* values were calculated using CMRTools/Thalassemia Tools software program, Cardiovascular Imaging Solutions, London, UK. In CMRtools, a region of cerebral cortex was chosen in the brain. All the pixels intensity within the ROI are averaged together and fitted to a monoexponential decay model; equation: $SI(TE) = A \times \exp(-TE / T2^*)$ where A is a constant, TE, echo time, and SI, signal intensity (Supplement data). The methods for calculated T2* values were modified from Anderson et al. and Bacigalupo et al. [23,24].

3.3. Measurement of brain tissues iron content

The levels of non-heme iron in the brain samples were determined using a modification of the ferrozine method described by [25]. Brain samples were homogenized in 1 ml of 0.1 M PBS buffer, pH 7.4. Iron was extracted by adding an equal volume of brain tissue homogenate (250 μl) and protein precipitants (125 μl of 1 N HCl and 125 μl of 10% trichloroacetic acid, Sigma). After mixing, the solution was incubated in a water bath at 95 °C for 45 min. An additional supernatant was then collected. [26]. To analyze the iron content, the supernatant was diluted with 1 N HCl to a total volume of 500 μl and further mixed with 1 ml of chromogen solution (0.5 mM ferrozine, 50 mM sodium ascorbate, and 1.05 M sodium acetate, Sigma). After 20 min incubation at room temperature, the absorbance was measured at 562 nm using the Thermo Scientific™ Varioskan™ Flash (Vantaa, Finland).

3.4. Histopathological studies

Brain samples were dissected and preserved for routine histology by fixation in 4% paraformaldehyde, 5% sucrose and 150 mM PBS, pH 7.4. The fixed tissues were dehydrated and embedded in paraffin, sectioned to 5 μm thick. Serial sections were stained with Hematoxylin and Eosin staining method (H&E) for morphological changes and with Perls' Prussian blue staining method for iron deposition by standard procedures [27]. The tissue slides were examined by light microscopy on a Nikon ECLIPSE E200 (Tokyo, Japan).

3.5. Statistical analysis

Statistical analysis was performed with SPSS software version 19.0. The data were expressed as the means ± SD unless otherwise indicated. The comparisons were analyzed by oneway analysis of variance (ANOVA) with Dunnett test as a post test. Pearson correlation as a correlation between brain iron content and brain T2* values MRI. Statistical significance was considered when the p-value < 0.05.

4. Results

4.1. Brain MRI: quantitative histogram analyses

In the iron overload group, the histogram analyses calculated from T2 weighted images of the 3 brain regions including cortex-cerebellar

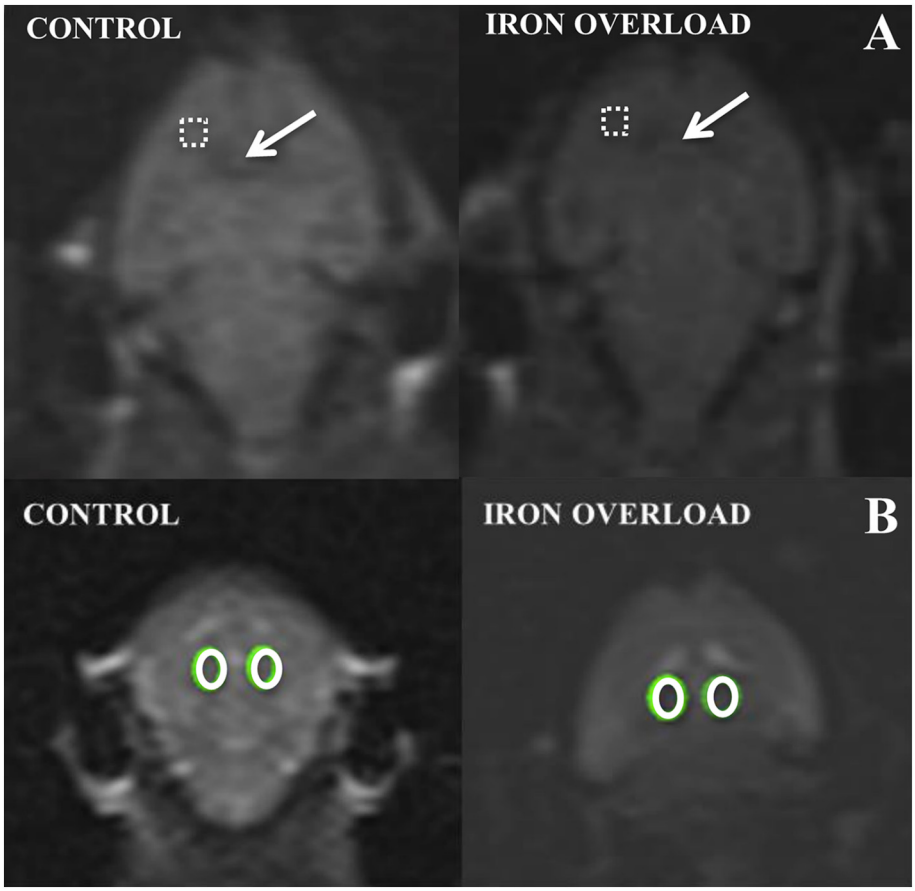

Fig. 1. Brain histogram analyses of the 3 brain regions including (A) cortex-cerebellar white matter (), hippocampus (), and (B) superior colliculus (). The total mean histogram of the regions was calculated from each slice in all mice and compared between the iron overloaded and control group.

white matter, superior colliculus, and hippocampus showed decreased signal intensity and an increase in the frequency of occurrence of pixels with shorter T2 values, consistent with increased ferritin iron. Loading of 100 mg of iron significantly decreased the mean histogram analyses in the superior colliculus and hippocampus of brain of β-thalassemic mice. Control group 30.43 ± 6.21, 15.43 ± 1.51, and 11.00 ± 1.00 for cortex-cerebellar white matter, superior colliculus, and hippocampus, respectively. Iron overloaded group 28.71 ± 5.62, 13.29 ± 1.25 ($p = 0.04$), and 8.57 ± 1.27 ($p = 0.006$) for cortex-cerebellar white matter, superior colliculus, and hippocampus, respectively. The MRI imaging demonstrated that the 3 regions of the brain of the iron overloaded group were hypointensity compared to the control mice (Fig. 1). However, treatment with deferiprone did not significantly change the mean histogram analyses of the 3 regions of interest in the brain of β-thalassemic mice (29.00 ± 4.20, 13.57 ± 0.79, and 8.71 ± 0.76 for cortex-cerebellar white matter, superior colliculus, and hippocampus, respectively).

4.2. Brain iron content and brain T2* values

The MRI imaging demonstrated that the regions of the brain were selected to analyze T2* values as shown in Fig. 2. Loading of 100 mg of iron significantly increased iron accumulation in the brain of β-thalassemic mice. The iron content was 7.76 ± 1.39 and 0.08 ± 0.00 mg/g tissue ($p = 0.001$) in iron overloaded and control mice, respectively. Treatment with deferiprone significantly reduced iron deposition in the brain of iron overloaded mice to 4.75 ± 0.63 mg/g tissue ($p = 0.021$) (Fig. 3a).

Corresponding to iron accumulation, the brain T2* value of the control group was 28.51 ± 4.53 ms, that of the iron overloaded group was 9.80 ± 0.94 ms ($p < 0.001$), and the value was significantly reverted to 17.87 ± 3.85 ms ($p = 0.008$) in the deferiprone treatment group (Fig. 3b). Pearson's correlation demonstrated that the brain T2* value had significant negative correlations with iron content parameters ($r = -0.872$, $p < 0.001$) (Fig. 3c).

4.3. Brain histopathology

4.3.1. Hematoxylin and eosin staining

Hematoxylin and eosin (H&E) stained coronal brain sections in the cerebral cortex of β-thalassemic mice as shown in Fig. 4a, b, c. In iron overload group, there was shown signs of large cells which are mostly multipolar, neuronal swelling, chromatolysis and nuclear margination (Fig. 4b). Hyperchromatic cells, vascular congestion in the cerebral cortex and cellular necrosis were observed (×400). However, treatment with deferiprone decreased the size of the foci, and they became more ellipsoidal than spherical in shape (Fig. 4c).

4.3.2. Prussian blue staining

Fig. 4d, e, f shows a representative image of the Prussian blue staining of the coronal brain sections in the cerebral cortex of β-thalassemic mice. Spontaneous iron deposition was observed in the brain β-thalassemic mice, shown in microglia cell (Fig. 4d). After iron loading, iron was found in several area of brain including cerebral cortex (Fig. 4e), cerebellum, and choroid plexus (data not shown). Treatment with deferiprone, found iron accumulation decreased in cerebral cortex (Fig. 4f).

5. Discussions

In this study, we demonstrated the utility of T2 weighted images and T2* values for quantification of brain iron, and effect iron chelator; deferiprone of in iron overloaded β-thalassemic mice model. In brain tissue, T2 shortening can be observed as hypointensity on T2 weighted

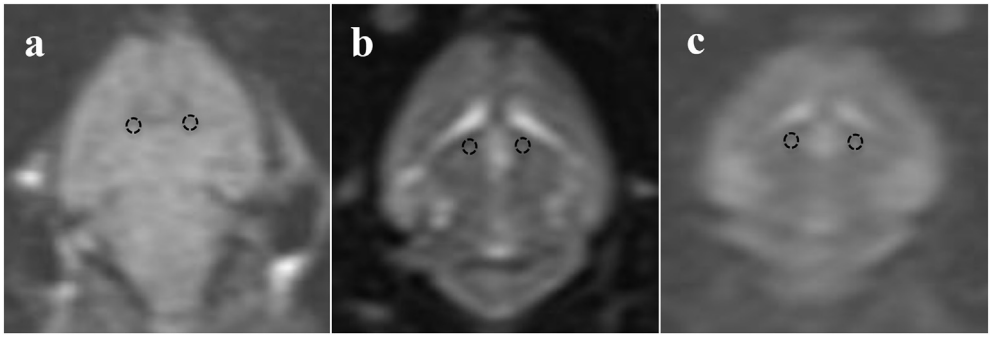

Fig. 2. Region of cerebral cortex was chosen in the brain. Mark areas identify the anatomical regions that the signal intensity was analyzed T2* value for each of the images and compared between control (a), the iron overloaded (b) and chelation group (c).

images and T2* values decreased due to with iron accumulation. The value was significantly increased in the group of the treatment of deferiprone. The change in T2* value had significant negative correlation with iron content in the brain.

Previous studies have shown that MRI was a useful parameter to quantify hepatic and cardiac iron concentrations in both humans [28–30] and animals [31]. Moreover, there was confirmed progression for the determination of brain iron concentration in aging adults and monkeys [32,33]. In heavy iron overload, iron is mainly stored in tissue in the form of hemosiderin, an insoluble and nontoxic state in addition to ferritin [34]. Several techniques have been developed that detect MR signal alterations derived mainly from the magnetic properties of hemosiderin [35].

In humans, T2* MRI is the primary technique for identifying pathological iron overload in thalassemia patients [36]. T2 has also been shown to be a useful and reproducible measure of tissue iron; however, T2* remains the gold standard due to the important number of validation studies [37]. The MR signal intensity was observed on routine clinical T2-weighted MRI sequences on a 1.5 T scanner. Brain histogram analysis calculated from T2 weighted images, was calculated on a pixel-by-pixel basis, which is the degree of distribution of iron overload and is a textural-based measure of the variation and probability of individual values in the overall histogram distribution of values across the region of interest. However, the iron brain histogram analysis is unwieldy and may not be practical in daily clinical practice.

Our study observed the decreased MRI signal intensity of the region of interest including cortex-cerebellar white matter, superior colliculus, and hippocampus. Cortex-cerebellar white matter is involved in the network dysfunction transmission process; abnormalities of this area were found in patients with major depressive disorders. Superior colliculus is involved in a wide variety of behaviors, generating spatially directed head turns and arm-reaching movements; abnormalities of this area were found in patients with Parkinson's disease. Patients present with parkinsonism, gait disturbances, and psychosis. The hippocampus is involved in learning and memory, and abnormalities of this area were found in patients with Alzheimer's disease. Therefore, iron accumulation in these areas may affect brain function. Several different mechanisms have been proposed as the cause of neurodegeneration in thalassemia disease including oxidative stress and mitochondrial dysfunction [38]. Iron has been implicated in the pathogenesis of several

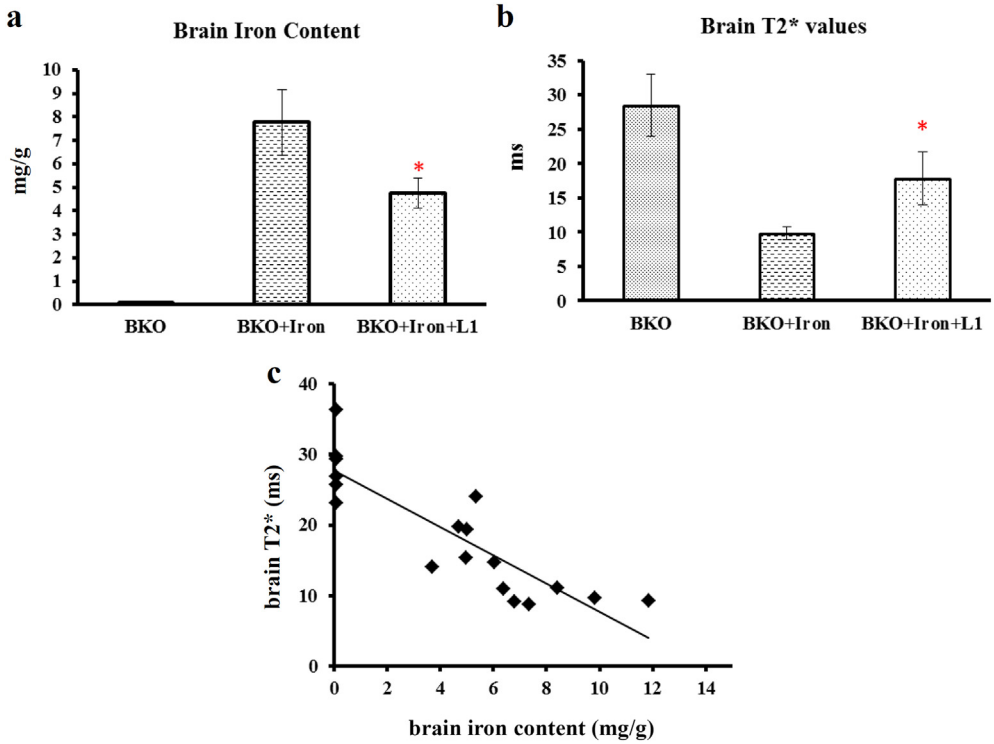

Fig. 3. Brain iron content of β-thalassemic mice, iron overloaded, deferiprone (a). Brain T2* values of β-thalassemic mice, iron overloaded, deferiprone (b). Relationship between brain iron content and brain T2* values (c). Brain iron content strongly correlates with results of brain T2* value ($R = -0.872$, $p < 0.001$).

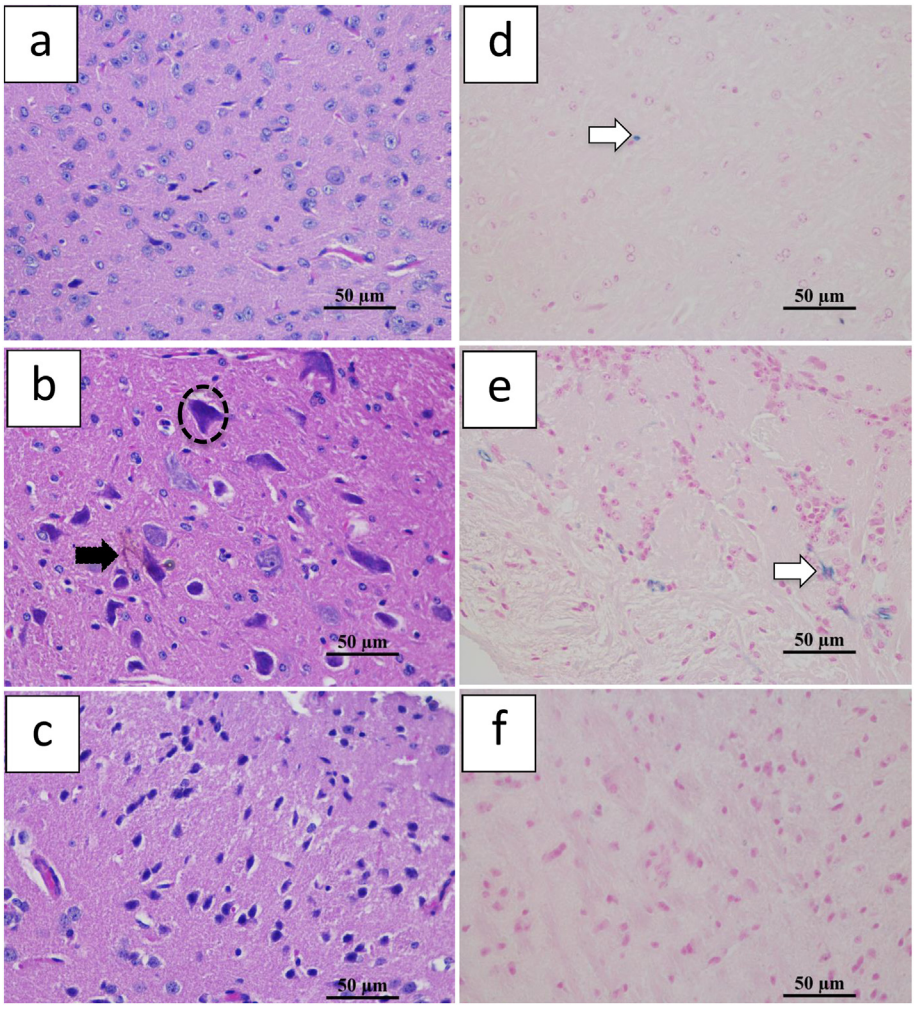

Fig. 4. Hematoxylin and eosin (a, b, c) and Prussian blue (d, e, f) staining of coronal brain sections of BKO mice. Control (a, d), iron overload (b, e) and iron-overloaded mice treated with deferiprone (c, f). The bar represents 50 μm, and the images were taken at 400× original magnification. Changes in morphology were observed in the iron-overloaded β-thalassemic mice, including the presence of clumps of brown pigment (➡) and neuronal swelling, chromatolysis and nuclear margination were observed in the cerebral cortex (◌). Treatment with deferiprone decreased the size of the neuronal cell. The iron accumulated primarily in the microglia cell (⇨). Treatment with iron chelators primarily removed iron from the microglia cell. (For interpretation of the references to color in this figure legend, the reader is referred to the web version of this article.)

neurodegenerative disorders due to its ability to generate cytotoxic reactive radicals that produce oxidative stress. Previous studies reported that acute neurological complications in patients with beta-thalassemia have been reported in association with cerebral ischemia, spinal cord fractures and compression from extramedullary hematopoietic tumors [39–42]. However, a pathogenic role of iron in the thalassemia brain is unclear.

Deferiprone, an iron chelator that may cross the blood–brain barrier and is able to remove excess iron from liver and heart [43]. Treatment with deferiprone in human, qualitative and quantitative evaluation of MRI showed that deferiprone was able to reduce brain iron accumulation in some patients, confirming previous observations in Friedreich's ataxia [44,45]. There are suggesting that the drug is apparently able to partially remove chelatable iron in different brain regions. This observation confirms the reduction in globus pallidus iron content, as assessed by T2* relaxometry, observed in 9 subjects treated with deferiprone (25 mg/kg/day) [46].

In conclusion, we demonstrated that MRI techniques and T2* value are useful for the detection of iron accumulation. Additionally, monitoring the effects of an iron chelator in the brain of β-thalassemic mouse models is the primary achievement and should be highlighted. Longitudinal studies in a larger number of β-thalassemic mice are needed to quantify brain iron accumulation using other post-processing techniques such as MRI relaxometry (R2, R2*) represents progressive iron accumulation and whether it represents degeneration progression in the brain. Furthermore, understanding brain function that is concerned with areas of iron accumulation is necessary to determine how iron regulation contributes to pathology in β-thalassemic mice.

Supplementary data to this article can be found online at https://doi.org/10.1016/j.mri.2019.05.022.

Acknowledgments

This work was supported by Research Grant No. MRG5980059 from the Thailand Research Fund (TRF) and the Office of Higher Education Commission; and by the Office of the Higher Education Commission and Mahidol University under the National Research Universities Initiative. Deferiprone was provided by the Government Pharmaceutical Organization, Bangkok, Thailand. The authors thank the Faculty of Veterinary Medicine, Kasetsart University for supporting the MRI for conducting this research.

References

[1] Stankiewicz J, Panter SS, Neema M, et al. Iron in chronic brain disorders: imaging and neurotherapeutic implications. Neurotherapeutics. 2007;4(3):371–86.
[2] Duce JA, Tsatsanis A, Cater MA, et al. Iron-export ferroxidase activity of beta-amyloid precursor protein is inhibited by zinc in Alzheimer's disease. Cell 2010;142:857–67.
[3] Becerril-Ortega J, Bordji K, Fréret T, et al. Iron overload accelerates neuronal amyloid-b production and cognitive impairment in transgenic mice model of Alzheimer's disease. Neurobiol Aging 2014:2288–301.
[4] Lee DW, Andersen JK. Role of HIF-1 in iron regulation: potential therapeutic strategy for neurodegenerative disorders. Curr Mol Med 2006;6(8):883–93.
[5] Blasco G, Puig J, Daunis-I-Estadella J, et al. Brain iron overload, insulin resistance, and cognitive performance in obese subjects: a preliminary MRI case-control study. Diabetes Care 2014;37(11):3076–83.
[6] Ott M, Stouffer C, Foote J, et al. Roux-en-Y gastric bypass: a novel approach to the treatment of hemochromatosis? Am J Hematol 2007;82(11):1033.

[7] Dixon ML, Christoff K. The decision to engage cognitive control is driven by expected reward-value: neural and behavioral evidence. PLoS One 2012;7(12):e51637.
[8] Papakonstantinou O, Alexopoulou E, Economopoulos N, et al. Assessment of iron distribution between liver, spleen,pancreas, bone marrow, and myocardium by means of R2 relaxometry with MRI in patients with beta-thalassemia major. J Magn Reson Imaging 2009;29:853–9.
[9] Metafratzi Z, Argyropoulou MI, Kiortsis DN, et al. T2 relaxation rate of basal ganglia and cortex in patients with beta-thalassaemia major. Br J Radiol 2001;74(881):407–10.
[10] Oerter KE, Kamp GA, Munson PJ, et al. Multiple hormone deficiencies in children with hemochromatosis. J Clin Endocrinol Metab 1993;76:357–61.
[11] Argyropoulou MI, Kiortsis DN, Metafratzi Z, et al. Pituitary gland height evaluated by MR in patients with beta-thalassemia major: a marker of pituitary gland function. Neuroradiology 2001;43:1056–8.
[12] Brittenham GM, Badman DG. Noninvasive measurement of iron: report of an NIDDK workshop. Blood 2003;101(1):15–9.
[13] Bartzokis G, Mintz J, Marx P, et al. Reliability of in vivo volume measures of hippocampus and other brain structures using MRI. Magn Reson Imaging 1993;11(7):993–1006.
[14] Khalil M, Teunissen C, Langkammer C. Iron and neurodegeneration in multiple sclerosis. Mult Scler Int 2011;2011:1–6.
[15] Bartzokis G, Sultzer D, Cummings J, et al. In vivo evaluation of brain iron in Alzheimer disease using magnetic resonance imaging. Arch Gen Psychiatry 2000;57(1):47–53.
[16] Brass SD, Benedict RH, Weinstock-Guttman B, et al. Cognitive impairment is associated with subcortical magnetic resonance imaging grey matter T2 hypointensity in multiple sclerosis. Mult Scler 2006;12:437–44.
[17] Thomas LO, Boyko OB, Anthony DC, et al. MR detection of brain iron. AJNR Am J Neuroradiol 1993;14(5):1043–8.
[18] Yang B, Kirby S, Lewis J, et al. A mouse model for β0-thalassemia.Proc Natl Acad Sci1995; 92,11608–11612.
[19] Jamsai D, Zaibak F, Khongnium W, et al. A humanized mouse model for a common beta-thalassemia mutation. Genomics 2005;85:453–61.
[20] Grabill C, Silva AC, Smith SS, et al. MRI detection of ferritin iron overload and associated neuronal pathology in iron regulatory protein-2 knockout mice. Brain Res 2003;971:95–106.
[21] Della Nave R, Foresti S, Pratesi A, et al. Whole-brain histogram and voxel-based analyses of diffusion tensor imaging in patients with leukoaraiosis: correlation with motor and cognitive impairment. AJNR Am J Neuroradiol 2007;28:1313–9.
[22] Blackledge MD, Collins DJ, Koh DM, Leach MO. Rapid development of image analysis research tools: bridging the gap between researcher and clinician with pyOsiriX. Comput Biol Med 2016;69:203–12.
[23] Anderson LJ, Westwood MA, Holden S, et al. Myocardial iron clearance during reversal of siderotic cardiomyopathy with intravenous desferrioxamine: a prospective study using T2* cardiovascular magnetic resonance. Br J Haematol 2004;127:348–55.
[24] Bacigalupo L, Paparo F, Zefiro D, et al. Comparison between different software programs and post-processing techniques for the MRI quantification of liver iron concentration in thalassemia patients. Radiol Med 2016;121:751–62.
[25] Foy AL, Williams HL, Cortell S, et al. A modified procedure for the determination of non-heme iron in tissue. Anal Biochem 1967;18:559–63.
[26] Yatmark P, Morales NP, Chaisri U, et al. Iron distribution and histopathological study of the effects of deferoxamine and deferiprone in the kidneys of iron overloaded β-thalassemic mice. Exp Toxicol Pathol 2016 Sep;68(8):427–34.
[27] Hall AP, Davies W, Stamp K, et al. Comparison of computerized image analysis with traditional semiquantitative scoring of Perls' Prussian Blue stained hepatic iron deposition. Toxicol Pathol 2013;41(7):992–1000.
[28] Wood JC. Magnetic resonance imaging measurement of iron overload. Curr Opin Hematol 2007;14(3):183–90.
[29] Wood JC, Ghugre N. Magnetic resonance imaging assessment of excess iron in thalassemia, sickle cell disease and other iron overload diseases. Hemoglobin. 2008;32(1–2):85–96.
[30] Wood JC, Noetzli L. Cardiovascular MRI in thalassemia major. Ann N Y Acad Sci 2010;1202:173–9.
[31] Goodall EF, Haque MS, Morrison KE. Increased serum ferritin levels in amyotrophic lateral sclerosis (ALS) patients. J Neurol 2008;255:1652–6.
[32] Haacke EM, Miao Y, Liu M, et al. Correlation of change in R2* and phase with putative iron content in deep gray matter of healthy adults. J Magn Reson Imaging 2010;32:561–76.
[33] Hardy PA, Gash D, Yokel R, et al. Correlation of R2 with total iron concentration in the brains of rhesus monkeys. J Magn Reson Imaging 2005;21:118–27.
[34] Carrondo MA. Ferritins, iron uptake and storage from the bacterioferritin viewpoint. EMBO J 2003 May 1;22(9):1959–68. [Review].
[35] Dusek P, Schneider SA. Neurodegeneration with brain iron accumulation. Curr Opin Neurol 2012;25(4):499–506.
[36] Pennell DJ, Udelson JE, Arai AE, et al. Cardiovascular function and treatment in β-thalassemia major: a consensus statement from the American Heart Association. Circulation. 2013;128(3):281–308.
[37] Pennell DJ. T2* magnetic resonance: iron and gold. JACC Cardiovasc Imaging 2008;1:5.
[38] Shaki F, Shayeste Y, Karami M, et al. The effect of epicatechin on oxidative stress and mitochondrial damage induced by homocycteine using isolated rat hippocampus mitochondria. Res Pharm Sci 2017 Apr;12(2):119–27.
[39] Sinniah D, Vignaendra V, Ahmad K. Neurological complications of beta-thalassaemia major. Arch Dis Child 1977;52(12):977–9.
[40] Issaragrisil S, Piankigagum A, Wasi P. Spinal cord compression in thalassemia. Report of 12 cases and recommendations for treatment. Arch Intern Med 1981;141(8):1033–6.
[41] Massenkeil G, Wichmann W, Krummenacher F, et al. Reversible spinal cord compression caused by extramedullary hematopoietic foci in thalassemia. Dtsch Med Wochenschr 1993;118(4):100–6.
[42] Aarabi B, Haghshenas M, Rakeii V. Visual failure caused by suprasellar extramedullary hematopoiesis in beta thalassemia: case report. Neurosurgery 1998;42(4):922–925; discussion 925–926.
[43] Yatmark P, Morales NP, Chaisri U, et al. Iron distribution and histopathological characterization of the liver and heart of β-thalassemic mice with parenteral iron overload: effect of deferoxamine and deferiprone. Exp Toxicol Pathol 2014;66:333–43.
[44] Boddaert N, Le Quan Sang KH, et al. Selective iron chelation in Friedreich ataxia: biologic and clinical implications. Blood. 2007;110(1):401–8.
[45] Kakhlon O, Breuer B, Munnich A, et al. Neurological disorders associated with iron misdistribution: the therapeutic potential of siderophores. In: Gadoth N, Goebel H, editors. Oxidative stress and free radical damage in neurology. 2011. p. 169–90.
[46] Zorzi G, Zibordi F, Chiapparini L, et al. Iron-related MRI images in patients with Pantothenate Kinase–Associated Neurodegeneration (PKAN)treated with Deferiprone: results of a phase II pilot trial. Mov Disord 2011;26(9):1756–9.